Finite-size effects in the microscopic structure of a hard-sphere fluid in a narrow cylindrical pore

F. L. Román
Departamento de Física Aplicada, Universidad de Salamanca, E-37008 Salamanca, Spain and Escuela Politécnica Superior de Zamora, Universidad de Salamanca, E-49022 Zamora, Spain

J. A. White,[a] A. González, and S. Velasco
Departamento de Física Aplicada, Universidad de Salamanca, E-37008 Salamanca, Spain

(Received 22 December 2005; accepted 21 February 2006; published online 19 April 2006)

We examine the microscopic structure of a hard-sphere fluid confined to a small cylindrical pore by means of Monte Carlo simulation. In order to analyze finite-size effects, the simulations are carried out in the framework of different statistical mechanics ensembles. We find that the size effects are specially relevant in the canonical ensemble where noticeable differences are found with the results in the grand canonical ensemble (GCE) and the isothermal isobaric ensemble (IIE) which, in most situations, remain very close to the infinite system results. A customary series expansion in terms of fluctuations of either the number of particles (GCE) or the inverse volume (IIE) allows us to connect with the results of the canonical ensemble. © *2006 American Institute of Physics*.
[DOI: 10.1063/1.2187487]

I. INTRODUCTION

Many recent advances in the understanding and control of materials come from the increasing ability to carry out manipulations at the molecular level. The rapid development of the science and technology of nanomaterials requires a deep understanding of the properties of small systems such as molecular size pores and nanotubes, thus becoming a subject of fundamental importance for physics and chemistry.[1] In this context, the study of fluids confined to simple geometries has been an object of great interest in the last few years because of the appearance of novel practical applications. Materials such as zeolites or porous glasses act as hosts for the molecules of a fluid absorbed in the pores of the confining solid material. The properties of the confined fluid and sometimes those of the host material can be altered in this process, becoming significantly different from the bulk.[2] For instance, the structure of confined freezed water has been recently shown to strongly depend on the confining geometry.[3,4]

Apart from their practical applications, strongly confined fluids have become the subject of a great deal of theoretical studies. An important theoretical aspect appears when the system consists of a very reduced number of particles, i.e., when one is dealing with a small system. In this case the statistical mechanics ensembles are no longer equivalent[5–9] and care must be taken in order to perform a correct study of the system. The statistical mechanics description of an equilibrium system with N particles in a volume V at temperature T is appropriately made in the framework of the canonical ensemble (CE). It is well known that for large systems, an equivalent description can be made in the grand canonical ensemble (GCE) or even in the isothermal isobaric ensemble (IIE). In the GCE the number of particles is allowed to fluctuate due to particle exchange with an external reservoir characterized by a chemical potential μ. Analogously, in the IIE the volume fluctuates because the system is subjected to a fixed external pressure P. These fluctuations either in N (GCE) or in V (IIE) are crucial in the study of systems with a very small number of particles where their influence can even modify the microscopic equilibrium structure of the system.[5–9] It is thus clear that the external conditions acting on a small system must be taken into account in order to determine the ensemble required for its statistical mechanics study. A basic tool for this study is Monte Carlo (MC) simulation which can be formulated in the different ensembles with similar computational effort.[10] In many situations the ensemble choice in a MC simulation is motivated by the above-mentioned external conditions for the system. In other cases, however, this election is not possible and one is obliged to work in a certain ensemble due to problems with statistical accuracy in another (perhaps more appropriate) ensemble. This is the case for classical fluids in the GCE at very high packings where the probability of particle exchange with the reservoir becomes close to zero and one needs very large simulation runs for obtaining results with good statistics. In this situation working with a fixed number of particles can be very useful and one can consider either the CE or the IIE.[10–12] In particular, an IIE approach for a small system is appealing due to the appearance of volume fluctuations. In this work we will see how under certain circumstances this ensemble yields results that are equivalent to those of the GCE. This fact can be of relevance in MC simulations where sometimes the GCE may present technical difficulties.[10] As an aside we note that the IIE presents certain theoretical advantages in the study of one-dimensional

[a]Electronic mail: white@usal.es

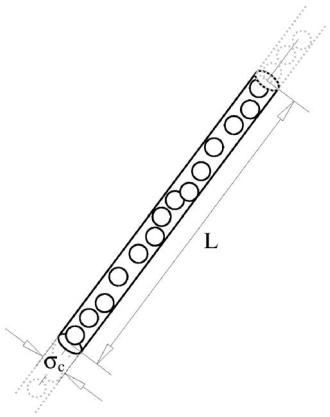

FIG. 1. Hard-sphere fluid in a narrow cylindrical pore.

systems[13,14] that can be also of interest for fluids confined in very narrow cylindrical pores,[15,16] specially in the extreme situation of single-file systems.[17,18]

The goal of this paper is to study the explicit finite-size effects that arise in the structure of a hard-sphere fluid confined to a narrow cylindrical pore due to the choice of a particular statistical mechanics ensemble. To this end, the paper is structured as follows. Section II presents the model system considered in this work with the details of the MC simulations in the different ensembles. In Sec. III we present our results for the density profile of the fluid. We link the results in the different ensembles by means of a series expansion in terms of fluctuations. In Sec. IV we consider an averaged two-body distribution function that yields information on the structure of the fluid along the axis of the cylinder. We conclude with a summary of the main results of the present work.

II. MODEL AND SIMULATION

Our system consists of a fluid of hard spheres of diameter σ confined to a hard cylindrical pore of diameter σ_c, i.e., the fluid is subjected to the following external potential:

$$V_{\text{ext}}(\mathbf{r}) = \begin{cases} 0, & r < \frac{1}{2}(\sigma_c - \sigma) \\ \infty, & r > \frac{1}{2}(\sigma_c - \sigma) \end{cases}, \tag{1}$$

where the radial coordinate r denotes the distance to the axis of the cylinder. We note that this expression for the external potential implies that the maximum distance from the axis to the center of the hard sphere is $\frac{1}{2}(\sigma_c - \sigma)$. To avoid border effects in the extremes of the cylindrical pore we consider the usual periodic boundary conditions. Also, because the external potential depends only on r, the density profile of the confined fluid must exhibit the same cylindrical symmetry. A sketch of the system is presented in Fig. 1.

In the present study we shall consider simulations in three different statistical mechanics ensembles, namely, the canonical ensemble, the grand canonical ensemble, and the isothermal isobaric ensemble, and thus we need different additional variables to define the system. In particular, in the CE we will consider a system with N spheres in a cylinder of fixed length L. This length is also fixed in the GCE but the number of particles fluctuates and we choose a chemical potential such that the average number of particles in the GCE $\langle N \rangle_{\text{GCE}}$ is equal to N and thus both systems have equal mean density. In order to have the same mean density also in the IIE, we consider an external pressure that yields an average inverse length $\langle L^{-1} \rangle_{\text{IIE}}$ equal to L^{-1} while N remains fixed (note that now $\langle \cdots \rangle_{\text{IIE}}$ indicates an average in the IIE).

The Monte Carlo simulations in the considered ensembles differ by the types of events allowed to occur in a simulation run (see, e.g., Ref. 10 for details). We note that the simulation procedures described below are adapted to a hard-particle system. In the CE simulation we only consider particle-move events: A randomly selected particle is given a random displacement. The move is accepted if the new particle position does not imply an overlap with another particle or with the cylinder walls, otherwise the old configuration is kept. In addition to this event, in the GCE we also consider a particle-insertion (removal) event in which with equal probability one tries to perform either the insertion or the removal of a particle from the system. A removal attempt is accepted with probability

$$\text{acc}(N \to N-1) = \min\left[1, \frac{N}{CV}\right], \tag{2}$$

where C is a quantity related to the chemical potential, and V is the volume in the pore accessible to the center of a particle, i.e., $V = \pi(\sigma_c - \sigma)^2 L/4$. Analogously, an insertion attempt is accepted with probability

$$\text{acc}(N \to N+1) = \min\left[1, \frac{CV}{N+1}\right]. \tag{3}$$

In this case, a newly created particle is located at a random position inside the pore. The insertion attempt is rejected if the new particle overlaps any of the other particles. Note that from a practical viewpoint, we can simulate a system with a given average number of particles by choosing an appropriate value of C.

In the IIE, instead of the insertion (removal) event, we consider a volume-change event. Since the external potential determines a fixed circular cross section for the cylindrical pore with area $A = \pi(\sigma_c - \sigma)^2/4$, the only allowed volume changes are those due to the variation of the length L of the system. In a volume-change attempt, a new length L' is proposed, and accepted with probability

$$\text{acc}(L \to L') = \min\left[1, \left(\frac{L'}{L}\right)^N \mathrm{e}^{-\beta PA(L'-L)}\right], \tag{4}$$

where $\beta = 1/k_B T$ is the inverse temperature and P is the external pressure. The volume change implies a scaling of the position of the particles along the axis of the cylinder; if this scaling leads to a particle overlap the volume-change attempt is rejected. Finally we note that the maximum allowed length increment in a volume-change attempt ($|\Delta L|_{\max}$) is chosen so that the overall acceptance ratio is about 30% of all attempts to perform a volume change. The same ratio is considered for the particle displacements.

While in the GCE simulation a Monte Carlo step (MCS) consists of selecting at random either a particle displacement or a particle insertion (removal), in the IIE one chooses a

displacement or a volume change with probabilities $N/(N+1)$ and $1/(N+1)$, respectively, for each MCS. Of course, in the CE every MCS is a particle displacement. In a typical simulation run we first equilibrate the system during $N \times 10^8$ MCs without performing measurements. Then we consider the same number of MCs in which we sample the averages of the quantities of interest every N MCs.

In the following two sections we present the results of our simulations. We first consider the density profile of the confined fluid, which, as mentioned above, exhibits the same cylindrical symmetry as the external potential and thus represents the radial structure of the system. Along the axis the density is homogeneous and we will consider an averaged two-body distribution function to show the important correlations that arise in the system, specially for very small cylinder diameters.

III. DENSITY PROFILES

The one-body distribution function or density profile $\rho(\mathbf{r})$ of an inhomogeneous fluid is defined as the ensemble average of the microscopic density,

$$\hat{\rho}(\mathbf{r}) = \sum_{i=1}^{N} \delta(\mathbf{r}_i - \mathbf{r}). \tag{5}$$

This implies that for any statistical mechanics ensemble, the density profile $\rho(\mathbf{r}) \equiv \langle \hat{\rho}(\mathbf{r}) \rangle$ of a fluid can be obtained by dividing the total volume in small subvolumes $v(\mathbf{r})$ and measuring the probability of having a particle in each $v(\mathbf{r})$. For a fluid confined in a cylindrical pore the profile is obtained by dividing the pore into concentric cylindrical shells, sampling the number of particles in each shell, and dividing by the volume of the shell.

In what follows we present the density profiles for the different statistical ensembles considered in this work, with the aim of investigating the finite-size effects that arise in the confined small system. For convenience we first start with the GCE which can be easily shown to yield results very close to those of an infinite system. We then compare with the CE and establish a link between both ensembles using a series expansion in terms of fluctuations in the number of particles (a well-known procedure). Finally we consider the IIE and connect with the other ensembles.

A. Grand canonical ensemble

It is not difficult to realize that our results for the GCE should be very close to those of an *equivalent* system in the *thermodynamic limit*. This equivalent infinite system must also be subjected to the external potential (1), and thus it becomes a fluid of $N_\infty \to \infty$ particles confined to a cylindrical pore of length $L_\infty \to \infty$ with finite mean density $\rho_m \equiv N_\infty / V_\infty$, where $V_\infty = AL_\infty$ is the volume available to the centers of the particles. In contrast, the corresponding small system in the GCE is a fluid with an average number of particles $\langle N \rangle$ in a volume $V=AL$ such that $\langle N \rangle / V = \rho_m$. The density profile for such system should differ very little from that of a fragment of length L of the infinite system which, given the cylindrical symmetry of the problem, exhibits the same profile as the infinite system itself. The main source of differences between the fragment and the small system comes from the periodic boundary conditions considered in the latter. However, the effect of the periodic boundary conditions is known to be negligible except for very special situations,[19] and thus we conclude by stating that in most situations the GCE profile is (almost) the same as that of an equivalent infinite system.

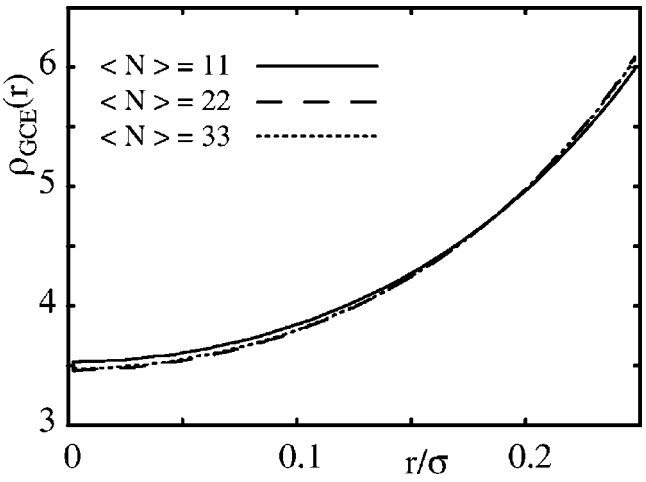

FIG. 2. Density profiles of hard spheres in a cylindrical pore of diameter $\sigma_c = 1.5\sigma$ in the GCE: $L=12\sigma$ and $\langle N \rangle = 11$ (solid line), $L=24\sigma$ and $\langle N \rangle = 22$ (dashed line), and $L=36\sigma$ and $\langle N \rangle = 33$ (dots).

A very simple test supporting this statement can be made by comparing the profiles for systems with equal external potential, the same mean density ρ_m, and different lengths, e.g., $L, 2L, 3L, \ldots$. If this statement is true, the density profiles must be equal. This test has been made for several situations and we have found appreciable differences only for cases with very small number of particles and very high packings, with an average number of particles very close to the maximum number that the cavity can hold. This special situation is depicted in Fig. 2 where we consider a pore with diameter $\sigma_c = 1.5\sigma$ and different lengths with the same mean density. In particular, we consider $L=12\sigma$, 24σ, and 36σ with $\langle N \rangle = 11$, 22, and 33, respectively. As one can observe only the case with $L=12\sigma$ and $\langle N \rangle = 11$ presents appreciable differences with the other cases. It should be remarked that this pore only can hold a maximum of 12 particles and we consider an average number of particles $\langle N \rangle = 11$. If we consider lower packings with the same diameter and lengths, for instance, systems with $\langle N \rangle = 10$, 20, and 30 (not shown), we do not obtain any appreciable difference among the three profiles. A possible explanation for the differences observed in the pore with 11 particles is based on the fact that the free volume for this system is very small, thus decreasing the probability of particle exchange with the external reservoir. This also implies that, in this case, the GCE result is very close to the CE one [see Figs. 3(c) and 4(c)]. As the system size increases ($N=22, 33, \ldots$) the total free volume increases and it becomes more probable to find space enough to accommodate a new particle in the confined system.

B. Canonical ensemble

For very small systems like the ones considered previously, the CE Monte Carlo simulations give results that are

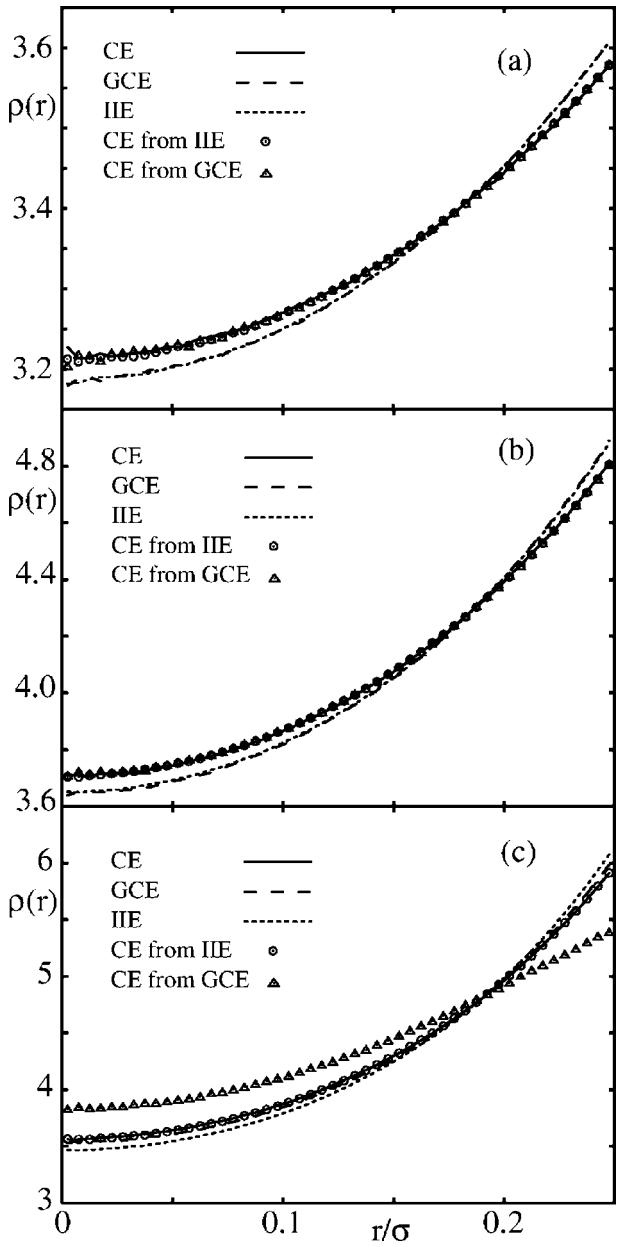

FIG. 3. Density profiles of hard spheres in a cylindrical pore of diameter $\sigma_c=1.5\sigma$ and inverse length $\langle 1/L\rangle=1/L=1/12\sigma^{-1}$: (a) $\langle N\rangle=N=8$, (b) $\langle N\rangle=N=10$, and (c) $\langle N\rangle=N=11$. The solid lines are the results of the CE simulations, the dashed lines correspond to GCE data, and the dots to IIE data. The symbols are the approximate CE results obtained from GCE (△) and IIE (⊙) data.

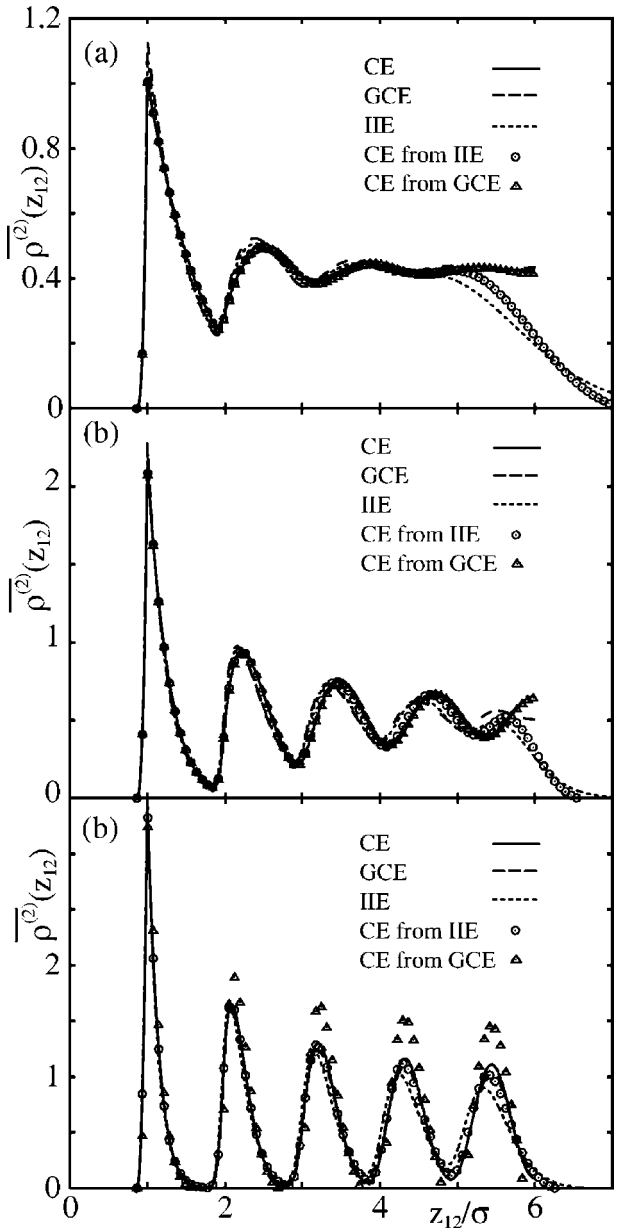

FIG. 4. Same caption as in Fig. 3 for the averaged two-body distribution function.

clearly different from those of the GCE. Since the latter are close to the density profile of an infinite cylindrical pore, one can conclude that it is in the CE where the finite-size effects play an important role. It is well known that these effects can be described by means of a series expansion in terms of fluctuations.[6,7,9] In particular, for the GCE density profile, one has[9]

$$\rho_{\mathrm{GCE}}(\mathbf{r}) = \rho_{\mathrm{CE}}(\mathbf{r}) + \frac{1}{2}\langle (N-\langle N\rangle)^2\rangle \frac{\partial^2}{\partial N^2}\rho_{\mathrm{CE}}(\mathbf{r}) + \frac{1}{6}\langle (N - \langle N\rangle)^3\rangle \frac{\partial^3}{\partial N^3}\rho_{\mathrm{CE}}(\mathbf{r}) + \cdots, \tag{6}$$

where the chemical potential in the GCE is chosen so that the mean number of particles $\langle N\rangle$ is equal to N, the number of particles in the CE. For a homogeneous system the CE density ρ_{CE} is equal to N/V and thus $\rho_{\mathrm{GCE}}=\rho_{\mathrm{CE}}$. However, for inhomogeneous situations, such as in the present cylindrical cavity, $\rho_{\mathrm{GCE}}(\mathbf{r})$ differs from $\rho_{\mathrm{CE}}(\mathbf{r})$, although the systems in both ensembles have the same mean density $\rho_m=N/V=\langle N\rangle/V$. From expansion (6), taking into account that the system volume V is constant, one can write

$$\rho_{\mathrm{GCE}}(\mathbf{r}) = \rho_{\mathrm{CE}}(\mathbf{r}) + \frac{1}{2N}\frac{\Delta^2(N)}{N}\rho_m^2\frac{\partial^2}{\partial \rho_m^2}\rho_{\mathrm{CE}}(\mathbf{r}) + O\left(\frac{1}{N^2}\right), \tag{7}$$

where $\Delta^2(N)\equiv\langle (N-\langle N\rangle)^2\rangle$ are the fluctuations in the number of particles in the system in the GCE. We note that in an infinite uniform system the fluctuations in the number of particles are equal to $\rho_m\langle N\rangle k_B T\chi_T$ where χ_T is the isothermal

compressibility. In the present inhomogeneous small system, following Lebowitz and Percus,[5] we can still write $\Delta^2(N)=\rho_m\langle N\rangle k_BT\bar{\chi}_T$, where $\bar{\chi}_T$ is certain average compressibility and thus

$$\rho_{\mathrm{GCE}}(\mathbf{r})=\rho_{\mathrm{CE}}(\mathbf{r})+\frac{1}{2N}\rho_m^3k_BT\bar{\chi}_T\frac{\partial^2}{\partial\rho_m^2}\rho_{\mathrm{CE}}(\mathbf{r})+O\left(\frac{1}{N^2}\right), \tag{8}$$

or, inverting formally the series, to order $O(1/N)$ one has

$$\rho_{\mathrm{CE}}(\mathbf{r})=\rho_{\mathrm{GCE}}(\mathbf{r})-\frac{1}{V}\phi(\rho_m), \tag{9}$$

where

$$\phi(\rho_m)=\frac{1}{2}\rho_m^2k_BT\bar{\chi}_T\frac{\partial^2}{\partial\rho_m^2}\rho_{\mathrm{GCE}}(\mathbf{r}) \tag{10}$$

is a function which [to order $O(1/N)$] does not depend on the size of the system [recall that $\rho_{\mathrm{GCE}}(\mathbf{r})$ is very close to $\rho_\infty(\mathbf{r},\rho_m)$ and thus $\partial^2\rho_{\mathrm{GCE}}(\mathbf{r})/\partial\rho_m^2=\partial^2\rho_\infty(\mathbf{r},\rho_m)/\partial\rho_m^2+O(1/N)$]. Therefore, the size effects for the density profile in the canonical ensemble scale with the (inverse) volume of the system and thus, in our cylindrical pore, with its length L. Expressions (7)–(10) determine the first-order contribution to the difference between the CE and GCE profiles. These expressions involve derivatives of profiles with different mean numbers of particles. The derivatives can be done numerically by considering simulations with different $\langle N\rangle$. It is more convenient, however, to rewrite the corrections in terms of fluctuations which can be measured in a single simulation run.[9] An explicit expression of Eq. (9) in terms of fluctuations is given in the Appendix [see Eq. (A8)].

In Fig. 3 we consider the density profiles for a pore with diameter $\sigma_c=1.5\sigma$ and length $L=12\sigma$ with $N=8$, 10, and 11 particles in the canonical ensemble. We compare with profiles in the GCE with $\langle N\rangle=8.00$, 10.00, and 11.00. We also consider the results of Eq. (A8). We observe that the differences between CE and GCE results decrease with increasing the number of particles. Also, for $N=8$ and 10, the differences are well described by Eq. (A8) while for $N=11$ the correction fails. This can be ascribed to the fact that the GCE density profile for the system with $\langle N\rangle=11.00$ differs from its corresponding infinite system profile (see Fig. 2 and above comments). In fact, if we had considered ρ_{GCE} in Eq. (A8) from a system with $\langle N\rangle=22.00$, $L=24\sigma$, and the same external potential, we would have obtained the CE profile ρ_{CE} for $N=11$ with the same degree of accuracy as in the cases $N=8$ and 10. Of course this would also work for larger systems. This means that, with obvious notation and to order $O(1/N)$, one can write

$$\rho_{\mathrm{CE}}(\mathbf{r})=\rho_\infty(\mathbf{r})-\frac{1}{V}\phi_\infty(\rho_m). \tag{11}$$

C. Isothermal isobaric ensemble

The connection between canonical and grand canonical results presented in the preceding subsection can be extended to the isothermal isobaric ensemble. Using a method analogous to that of Ref. 9 one can express the IIE density profile $\rho_{\mathrm{IIE}}(\mathbf{r})\equiv\langle\hat{\rho}(\mathbf{r})\rangle_{\mathrm{IIE}}$ as a series expansion in terms of fluctuations. The expansion is based on the fact that the IIE profile can be expressed as a volume average of the CE density profile, i.e.,

$$\rho_{\mathrm{IIE}}(\mathbf{r})=\int_0^\infty dV\omega(V)\rho_{\mathrm{CE}}(\mathbf{r},V), \tag{12}$$

where we have made explicit the V dependence of ρ_{CE}, and $\omega(V)$ is the volume probability density [see Eq. (A2) in the Appendix]. Expanding $\rho_{\mathrm{CE}}(\mathbf{r},\nu)$ about the mean inverse volume $\langle\nu\rangle$ and taking into account that $\omega(V)$ is normalized to 1, we obtain

$$\rho_{\mathrm{IIE}}(\mathbf{r})=\rho_{\mathrm{CE}}(\mathbf{r})+\frac{1}{2}\langle(\nu-\langle\nu\rangle)^2\rangle\frac{\partial^2}{\partial\nu^2}\rho_{\mathrm{CE}}(\mathbf{r})+\frac{1}{6}\langle(\nu-\langle\nu\rangle)^3\rangle\frac{\partial^3}{\partial\nu^3}\rho_{\mathrm{CE}}(\mathbf{r})+\cdots, \tag{13}$$

where now $\langle\cdots\rangle$ denotes IIE average and the pressure is chosen so that the mean inverse volume $\langle\nu\rangle$ is equal to ν, the inverse volume in the CE, and $\rho_{\mathrm{CE}}(\mathbf{r})=\rho_{\mathrm{CE}}(\mathbf{r},\langle\nu\rangle)$. A direct consequence of expansion (13) is that for a homogeneous system, $\rho_{\mathrm{CE}}=N/V=N\nu$ is equal to $\rho_{\mathrm{IIE}}=\langle N/V\rangle=N\langle\nu\rangle$. Of course this is due to the fact that the expansion is made about $\langle\nu\rangle$ and not about $\langle V\rangle$. It is important to remark that this simply means that we are comparing two systems in different ensembles so that the inverse volume in the CE, ν, is equal to the mean inverse volume in the IIE, $\langle\nu\rangle$, while $\langle V\rangle\neq V$. This choice implies that, in agreement with the homogeneous case, for an inhomogeneous situation one can define a mean density in the IIE $\rho_m=N\langle\nu\rangle$ so that it is equal to the mean density in the canonical and the grand canonical ensembles. Accordingly, we can rewrite (13) in the following form;

$$\rho_{\mathrm{IIE}}(\mathbf{r})=\rho_{\mathrm{CE}}(\mathbf{r})+\frac{1}{2}\frac{\Delta^2(\nu)}{\langle\nu\rangle^2}\rho_m^2\frac{\partial^2}{\partial\rho_m^2}\rho_{\mathrm{CE}}(\mathbf{r})+O(\nu^2), \tag{14}$$

where the derivatives are done at a constant number of particles. If we next consider for $\langle V\rangle$ and $\langle V^2\rangle$ an expansion similar to (13), it is not difficult to show that $\Delta^2(V)\equiv\langle(V-\langle V\rangle)^2\rangle\sim\Delta^2(\nu)/\langle\nu\rangle^4$. Furthermore, in an infinite uniform system the volume fluctuations are linked to the isothermal compressibility via $\Delta^2(V)/\langle V\rangle=k_BT\chi_T$. Thus, like in Eq. (8), for the present finite inhomogeneous system we can write $\Delta^2(\nu)/\langle\nu\rangle^3=k_BT\bar{\bar{\chi}}_T+O(\nu)$ where $\bar{\bar{\chi}}_T$ is an average compressibility. Comparing with Eq. (8), in general we expect $\bar{\bar{\chi}}_T=\bar{\chi}_T+O(\nu)$. Also, since $\rho_{\mathrm{CE}}=\rho_{\mathrm{GCE}}+O(\nu)=\rho_\infty+O(\nu)$ and ρ_∞ only depends on N or V through ρ_m, one has that the derivative $\partial^2\rho_{\mathrm{CE}}(\mathbf{r})/\partial\rho_{\mathrm{m}}^2$ at constant N that appears in Eq. (14) only differs by terms of order $O(\nu)$ from the derivative $\partial^2\rho_{\mathrm{GCE}}(\mathbf{r})/\partial\rho_{\mathrm{m}}^2$ at constant V of Eq. (8) and thus, Eq. (14) yields

$$\rho_{\mathrm{IIE}}(\mathbf{r})=\rho_{\mathrm{GCE}}(\mathbf{r})+O(\nu^2)=\rho_\infty(\mathbf{r})+O(\nu^2), \tag{15}$$

that is, $\rho_{\mathrm{IIE}}(\mathbf{r})$ differs from the GCE profile only by terms of order $O(\nu^2)$ and thus, measuring this quantity in the isothermal isobaric ensemble—even for small systems—yields an

accurate estimation of the infinite system inhomogeneous density. Finally we would like to remark that Eq. (14) can be formally inverted to yield

$$\rho_{\mathrm{CE}}(\mathbf{r}) = \rho_{\mathrm{IIE}}(\mathbf{r}) - \frac{1}{2}\frac{\Delta^2(\nu)}{\langle\nu\rangle^2}\rho_m^2\frac{\partial^2}{\partial\rho_m^2}\rho_{\mathrm{IIE}}(\mathbf{r}) + O(\nu^2), \tag{16}$$

which allows to obtain the CE profile from $\rho_{\mathrm{IIE}}(\mathbf{r})$.

At this point it is important to comment on the procedure used in the IIE simulation for measuring the density profile. In accordance with the series expansion proposed in (13), the simulation is made at an external pressure such that the mean value of the inverse volume is equal to the inverse volume in the CE, i.e., $\langle\nu\rangle = 1/V$. Then ρ_{IIE} is measured by dividing the cylindrical pore into concentric shells, sampling the number of particles in each shell and dividing by the volume of the shell. This volume is the product of the length L times the area $S(r)$ of the circular cross section of the shell. For a given shell, the area $S(r)$ is constant but L fluctuates through a simulation run, and thus the volume of the shell $v(r) = S(r)L$ also fluctuates, this being a crucial fact in the measurement of the isothermal isobaric profile.

The equivalence of $\rho_{\mathrm{IIE}}(\mathbf{r})$ with $\rho_{\mathrm{GCE}}(\mathbf{r})$ obtained in Eq. (15) is shown in Fig. 3 where in addition to the previously commented CE and GCE profiles we also plot the density profile for a pore with diameter $\sigma_c = 1.5\sigma$ and mean inverse length $\langle 1/L\rangle_{\mathrm{IIE}} = 1/L = 1/12\sigma^{-1}$ with $N=8$, 10, and 11 particles in the isothermal isobaric ensemble. We also show the approximate CE profile obtained from $\rho_{\mathrm{IIE}}(\mathbf{r})$ and Eq. (A7). For $N=8$ and 10 [Figs. 3(a) and 3(b)] we find excellent agreement between $\rho_{\mathrm{IIE}}(\mathbf{r})$ and $\rho_{\mathrm{GCE}}(\mathbf{r})$, and also between the CE profiles and the approximate results for $\rho_{\mathrm{CE}}(\mathbf{r})$ obtained both from $\rho_{\mathrm{IIE}}(\mathbf{r})$ and from $\rho_{\mathrm{GCE}}(\mathbf{r})$. For $N=11$ [Fig. 3(c)], however, we obtain important differences between the profiles. In particular, we would like to remark the following points for the $N=11$ case: (i) $\rho_{\mathrm{IIE}}(\mathbf{r})$ differs from $\rho_{\mathrm{GCE}}(\mathbf{r})$ due to finite-size effects in the GCE profile but agrees with the infinite system result (not shown, see Fig. 2 and comments), (ii) the approximate result for $\rho_{\mathrm{CE}}(\mathbf{r})$ obtained from $\rho_{\mathrm{IIE}}(\mathbf{r})$ agrees nicely with the CE profile, but (iii) the approximate result for $\rho_{\mathrm{CE}}(\mathbf{r})$ obtained from $\rho_{\mathrm{GCE}}(\mathbf{r})$ fails to yield the correct CE profile.

In summary, in all situations (including high packing) the IIE simulation data are very close to the infinite system results. This fact can be of particular relevance in situations like the one depicted in Fig. 3(c) where the GCE simulation data differ from the infinite system results due to the packing constraints in the system. This suggests the use of IIE simulations in situations where the GCE MC simulations present technical difficulties with insertion/removal events.

IV. AVERAGED TWO-BODY DISTRIBUTION FUNCTION

The density profiles presented in the preceding section only give information on the radial structure of the fluid confined to a cylindrical pore. Our goal now is to investigate the microscopic structure of the fluid along the axis of the pore. In this case the density is constant (unless a phase transition occurs) and one must consider the two-body distribution function of the fluid, $\rho^{(2)}$, which can be defined as follows:

$$\rho^{(2)}(\mathbf{r}_1,\mathbf{r}_2) \equiv \langle\hat{\rho}^{(2)}(\mathbf{r}_1,\mathbf{r}_2)\rangle = \left\langle \sum_{i\neq j=1}^{N} \delta(\mathbf{r}_i-\mathbf{r}_1)\delta(\mathbf{r}_j-\mathbf{r}_2)\right\rangle. \tag{17}$$

Strictly speaking, the structure in the axis of the pore is given by $\rho^{(2)}(x_1=0,y_1=0,z_1,x_2=0,y_2=0,z_2)$. It seems more convenient, however, to consider the average of $\rho^{(2)}$ over the *transverse* coordinates (x,y) so that we can define the following averaged distribution function:

$$\overline{\rho^{(2)}}(z_1,z_2) \equiv \int dx_1dy_1\int dx_2dy_2\rho^{(2)}(\mathbf{r}_1,\mathbf{r}_2) = \left\langle \sum_{i\neq j=1}^{N} \delta(z_i-z_1)\delta(z_j-z_2)\right\rangle, \tag{18}$$

which yields information on the average microscopic structure of the fluid along the cylinder. In particular, $\overline{\rho^{(2)}}(z_1,z_2)dz_1dz_2$ is the probability of finding one particle between z_1 and z_1+dz_1 and another particle between z_2 and z_2+dz_2. Due to translational invariance, $\overline{\rho^{(2)}}$ only depends on the distance $z_{12}\equiv|z_1-z_2|$, i.e., one has $\overline{\rho^{(2)}}(z_1,z_2)=\overline{\rho^{(2)}}(z_{12})$. After a standard change of variables and an integration, for a fixed cylinder length L, one obtains that the probability of finding a pair of particles with z coordinates separated a distance between z_{12} and $z_{12}+dz_{12}$ is given by $L\overline{\rho^{(2)}}(z_{12})dz_{12}$. This implies that $\overline{\rho^{(2)}}(z_{12})$ can be readily obtained in a simulation run by sampling the number of pairs of particles with a given separation z_{12} weighted by a factor $1/L$. This weight is not important in the CE or in the GCE but becomes crucial in the IIE where the length fluctuates.

Following the method presented in the preceding section for $\rho(\mathbf{r})$, it is not difficult to obtain approximate expressions that link the results for $\overline{\rho^{(2)}}$ in the different ensembles. In particular, the connection between the canonical and grand canonical ensembles is given by the analogous of Eq. (8):

$$\overline{\rho^{(2)}}_{\mathrm{GCE}}(z_{12}) = \overline{\rho^{(2)}}_{\mathrm{CE}}(z_{12}) + \frac{1}{2N}\rho_m^3k_BT\overline{\chi}_T\frac{\partial^2}{\partial\rho_m^2}\overline{\rho^{(2)}}_{\mathrm{CE}}(z_{12}) + O\left(\frac{1}{N^2}\right), \tag{19}$$

while for the IIE we obtain [see Eq. (14)]

$$\overline{\rho^{(2)}}_{\mathrm{IIE}}(z_{12}) = \overline{\rho^{(2)}}_{\mathrm{CE}}(z_{12}) + \frac{1}{2}\langle\nu\rangle\rho_m^2k_BT\overline{\chi}_T\frac{\partial^2}{\partial\rho_m^2}\overline{\rho^{(2)}}_{\mathrm{CE}}(z_{12}) + O(\nu^2), \tag{20}$$

and thus

$$\overline{\rho^{(2)}}_{\mathrm{IIE}}(z_{12}) = \overline{\rho^{(2)}}_{\mathrm{GCE}}(z_{12}) + O(\nu^2). \tag{21}$$

Figure 4 shows the behavior of $\overline{\rho^{(2)}}(z_{12})$ for a cylindrical pore of diameter $\sigma_c=1.5\sigma$ with $\langle 1/L\rangle = 1/L = 1/12\sigma^{-1}$, and $\langle N\rangle = N = 8$, 10, and 11, i.e., the same situations as those considered in Fig. 3 for the inhomogeneous density. We present the simulation results for the three ensembles considered in

the present work as well as the corresponding approximations for $\overline{\rho_{\mathrm{CE}}^{(2)}}(z_{12})$ based on the GCE and the IIE results.

Since the simulated system is subjected to periodic boundary conditions, the results for $\overline{\rho^{(2)}}(z_{12})$ are only valid for the range $0<z_{12}<L/2$ and, therefore, in Fig. 4 we only consider results up to $L/2=6\sigma$. Also, since the length L is a fluctuating variable in the IIE simulations, the results for $\overline{\rho_{\mathrm{IIE}}^{(2)}}$ near $\langle L\rangle/2$ exhibit an unphysical tail that must not be taken into account. The origin of this tail is clear: for a given value of the fluctuating length L one can only sample distances up to $L/2$ that can be smaller than the mean $\langle L\rangle/2$ giving rise to the tail, that can be seen as a further consequence of the periodic boundary conditions in the system.

In Fig. 4(a) we plot the results for the case $\langle N\rangle=N=8$. As expected, we find that GCE and IIE results are almost indistinguishable (except for the above-mentioned tail) while noticeable differences are found with the CE results. The approximations for $\overline{\rho_{\mathrm{CE}}^{(2)}}(z_{12})$ based on GCE and IIE data yield rather good results which shows the accuracy of the series expansions considered in this work. Figure 4(b) displays the results for $\langle N\rangle=N=10$ with the same overall behavior as in the preceding case but with a more pronounced peak structure. This structure is further enhanced in Fig. 4(c) where we plot the results for $\langle N\rangle=N=11$. This case corresponds to a very inhomogeneous situation where the CE and IIE results show the same behavior as in Figs. 4(a) and 4(b) while the GCE probability density $\overline{\rho_{\mathrm{GCE}}^{(2)}}$ is close to the CE result instead of the IIE one. Also, the approximation for $\overline{\rho_{\mathrm{CE}}^{(2)}}$ based on the GCE results fails noticeably. This situation is the same as the one presented in the preceding section for the density profile [see Fig. 3(c)] and, again, using results for an equivalent infinite system in the GCE (not shown), one would recover the behavior observed for the less inhomogeneous situations with $N=8$ and 10 particles.

To conclude, in this section we have analyzed the finite-size effects that arise in the averaged two-body distribution function $\overline{\rho^{(2)}}(z_{12})$, obtaining the same behavior as for the density profile: (i) in most situations IIE and GCE results are almost equal and differ from the CE results and (ii) good approximations for the CE results can be obtained on the basis of a series expansion in terms of fluctuations.

V. SUMMARY

We have analyzed the explicit finite-size effects that arise in the microscopic structure of a hard-sphere fluid in a narrow cylindrical pore when studied via MC simulation in the framework of different statistical mechanics ensembles. We have considered both the inhomogeneous density profile exhibited by the fluid in the radial direction and an averaged two-body distribution function that yields information on the structure along the axis of the cylindrical pore. In both cases we have observed that except for very small and highly inhomogeneous systems, the results in the GCE are very close to those of an equivalent infinite system. Conversely, the results in the CE differ from those in the GCE by a term of the order $O(1/N)$. An explicit expression for this term has been obtained by means of a series expansion in terms of the fluctuations in the number of particles.

In IIE, the choice of the system pressure becomes crucial. Instead of choosing a pressure such that the mean volume of the system is equal to that of the CE or GCE system we have considered a system whose mean inverse volume is equal to the inverse volume in the other ensembles. This choice has the direct consequence of yielding the same density for a homogeneous fluid in the three ensembles analyzed in this work. In the inhomogeneous situation considered in the present paper, a series expansion in terms of the inverse volume allowed us to show that the results in the IIE are equal to first order to those of the GCE and thus to the infinite system results. This theoretical result has been checked by MC simulation. This *equivalence* is remarkable given the size of the systems considered ($N\sim 10$) and taking into account that the equivalence with the infinite system holds even when the GCE simulation yields different results. Finally, the proposed series expansion can be used to link CE results to those in the IIE.

ACKNOWLEDGMENTS

This work was supported by *Ministerio de Ciencia y Tecnología* of Spain under Grant Nos. BFM2003-07106 FEDER and BFM2002-01225 FEDER, and by *Junta de Castilla y León* under Grant No. SA092/04.

APPENDIX: EQUATIONS IN TERMS OF FLUCTUATIONS

In this appendix we present the relevant expressions that allow one to rewrite the equations linking the results for the different ensembles in terms of fluctuations instead of derivatives with respect to the mean density. We first consider the IIE case and then quote the final results for the GCE which were already derived in a previous work.[9]

The IIE average $\langle A\rangle_{\mathrm{IIE}}$ of a given physical observable A can be expressed as the following volume average:

$$\langle A\rangle_{\mathrm{IIE}}=\int_0^\infty dV\omega(V)\langle A\rangle_{\mathrm{CE}}, \tag{A1}$$

where the volume probability density $\omega(V)$ is given by

$$\omega(V)=\frac{Q_{N,V}}{\delta_V\Delta_{N,P}}e^{-\beta PV}, \tag{A2}$$

$Q_{N,V}$ and $\Delta_{N,P}$ being the CE and the IIE partition functions, respectively, and δ_V is a volume scale that ensures that $\Delta_{N,P}$ is a dimensionless quantity. Differentiation of Eq. (A1) with respect to $-\beta P$ yields

$$\frac{\partial\langle A\rangle}{\partial(-\beta P)}=\langle AV\rangle-\langle A\rangle\langle V\rangle=\langle(A-\langle A\rangle)(V-\langle V\rangle)\rangle, \tag{A3}$$

where $\langle\cdots\rangle$ denotes IIE average. Differentiating again we obtain the following general expression:

$$\frac{\partial^n\langle A\rangle}{\partial(-\beta P)^n}=\langle(A-\langle A\rangle)(V-\langle V\rangle)^n\rangle, \tag{A4}$$

which is the key result for rewriting expressions with derivatives in terms of fluctuations. The derivatives with respect to

$\langle \nu \rangle = \langle V^{-1} \rangle$ are easily rearranged by taking into account the identity

$$\frac{\partial}{\partial \langle \nu \rangle} = \left(\frac{\partial \langle \nu \rangle}{\partial (-\beta P)} \right)^{-1} \frac{\partial}{\partial (-\beta P)}, \tag{A5}$$

where, using Eq. (A3),

$$\frac{\partial \langle \nu \rangle}{\partial (-\beta P)} = 1 - \langle \nu \rangle \langle V \rangle. \tag{A6}$$

Using Eqs. (A3)–(A6) to order $O(\nu)$ Eq. (16) becomes

$$\rho_{\mathrm{CE}}(\mathbf{r}) = \rho_{\mathrm{IIE}}(\mathbf{r}) - \frac{1}{2}\Delta^2(\nu)\left(\frac{\langle (\hat{\rho} - \rho_{\mathrm{IIE}})(V - \langle V \rangle)^2 \rangle}{\langle (\nu - \langle \nu \rangle)(V - \langle V \rangle) \rangle^2} - \frac{\langle (\hat{\rho} - \rho_{\mathrm{IIE}})(V - \langle V \rangle) \rangle \langle (\nu - \langle \nu \rangle)(V - \langle V \rangle)^2 \rangle}{\langle (\nu - \langle \nu \rangle)(V - \langle V \rangle) \rangle^3} \right), \tag{A7}$$

and a similar equation applies for $\overline{\rho^{(2)}}$.

The link between the GCE and the CE densities given by Eq. (9) can be rewritten in terms of fluctuations in the following way:[9]

$$\rho_{\mathrm{CE}}(\mathbf{r}) = \rho_{\mathrm{GCE}}(\mathbf{r}) - \frac{1}{2}\left(\frac{\langle (\hat{\rho} - \rho_{\mathrm{GCE}})(N - \langle N \rangle)^2 \rangle}{\Delta^2(N)} - \frac{\langle (\hat{\rho} - \rho_{\mathrm{GCE}})(N - \langle N \rangle) \rangle \langle (N - \langle N \rangle)^3 \rangle}{(\Delta^2(N))^2} \right). \tag{A8}$$

[1] L. D. Gelb, K. E. Gubbins, D. Radakrishman, and M. Sliwinska-Bartkowiak, Rep. Prog. Phys. **62**, 1573 (1999).
[2] R. Evans, J. Phys.: Condens. Matter **2**, 8989 (1990).
[3] I. Brovchenko, A. Geiger, and A. Oleinikova, J. Chem. Phys. **120**, 1958 (2004).
[4] K. Koga, G. T. Gao, H. Tanaka, and X. C. Zeng, Physica A **314**, 462 (2002).
[5] J. L. Lebowitz and J. K. Percus, Phys. Rev. **122**, 1675 (1961); **124**, 1673 (1961).
[6] J. L. Lebowitz, J. K. Percus, and L. Verlet, Phys. Rev. **153**, 250 (1967).
[7] J. J. Salacuse, A. R. Denton, and P. A. Egelstaff, Phys. Rev. E **53**, 2382 (1996).
[8] A. González, J. A. White, F. L. Román, S. Velasco, and R. Evans, Phys. Rev. Lett. **79**, 2466 (1997); J. A. White, A. González, F. L. Román, and S. Velasco, *ibid.* **84**, 1220 (2000).
[9] A. González, J. A. White, F. L. Román, and R. Evans, J. Chem. Phys. **109**, 3637 (1998).
[10] D. Frenkel and B. Smit, *Understanding Molecular Simulation. From Algorithms to Applications* (Academic, London, 1996).
[11] P. Attard, J. Chem. Phys. **103**, 9884 (1995).
[12] A. González, J. A. White, F. L. Román, and S. Velasco, J. Chem. Phys. **120**, 10634 (2004).
[13] H. Ted Davis, J. Chem. Phys. **93**, 4339 (1990).
[14] C. Tutschka and J. A. Cuesta, J. Stat. Phys. **111**, 1125 (2003).
[15] K. Kagannathan and A. Yethiraj, J. Chem. Phys. **116**, 5795 (2002).
[16] K. K. Mon and J. K. Percus, J. Chem. Phys. **117**, 2289 (2002).
[17] J. K. Percus, Mol. Phys. **100**, 2417 (2002).
[18] J. K. Percus, J. Stat. Phys. **15**, 505 (1976).
[19] L. R. Pratt and S. W. Haan, J. Chem. Phys. **74**, 1864 (1981); **74**, 1873 (1981); A. R. Denton and P. A. Egelstaff, Z. Phys. B: Condens. Matter **103**, 343 (1997); F. L. Román, J. A. White, A. González, and S. Velasco, J. Chem. Phys. **110**, 9821 (1999).